International Journal of Computer Information Systems and Industrial Management Applications
ISSN 2150-7988 Volume 18(6s) 2026 pp. 475-485
https://doi.org/10.70917/ijcisim-2026-2949
Article

A Comprehensive Deep Learning Framework for Diabetic Retinopathy Severity Grading: Integration of LDA-Based Segmentation and DenseNet121

K.Geethalakshmi

Dept. of BCA, PSGR Krishnammal College for Women Coimbatore, Tamilnadu, India.

Abstract: — Diabetic Retinopathy (DR) is a progressive retinal disorder caused by diabetes that can lead to irreversible vision loss if not detected early. This study aims to develop a reproducible deep learning workflow for the early detection and severity grading of DR. The proposed framework integrates image enhancement, lesion segmentation using Linear Discriminant Analysis (LDA), and a transfer learning classifier based on DenseNet121. Evaluation was conducted on a synthesized multi-source retinal fundus image dataset comprising EyePACS, APTOS, Messidor, and IDRiD. Experimental results demonstrate that segmentation-guided pre-processing significantly improves lesion visibility and enhances classification performance across DR severity levels. The model achieved sensitivity ranging from 71% to 90%, specificity ranging from 95% to 96%, and accuracy ranging from 92% to 95%. These findings indicate that the proposed approach offers reliable automated DR screening, with strong potential for clinical application and translation into real-world healthcare settings.

Keywords: Diabetic Retinopathy, Linear Discriminant Analysis, DenseNet121.

1. Introduction

Diabetic Retinopathy (DR) presents a significant public health concern. In industrialized nations, this long-term eye condition is one of the leading cause of blindness. DR is a diabetes-induced retinal disorder that gradually damages the blood vessels and affects vision. Research suggests that early detection and treatment help to prevent vision impairment up to 90% of cases. However, diagnosing DR traditionally relies on manual analysis of retinal images by physicians.

Retinal image processing is at the forefront of identifying and diagnosing numerous ocular illnesses, exploited superior imaging technology to lighten up the intricacies of the retina. Imaging abnormalities in the retina have provided early warning of diseases including age-related macular degeneration, glaucoma, and diabetic retinopathy because of the retina's special ability to provide diagnostic information about systemic health. Although modern imaging methods are often the center of attention, it's vital to be aware of their current capabilities and inherent limitations[24]. Fig. 1 represents the normal and DR affected retinal images. DR, Impairment or loss of vision, depending on the degree of the condition, may be caused by diabetic eye disease, which destroys the retina's capillary veins and nerve layer. Hard exudates, Microaneurysm, and hemorrhages are some of the lesions that might aid in the early detection of DR, If these retinal lesions are discovered early on, the condition may be more easily diagnosed.

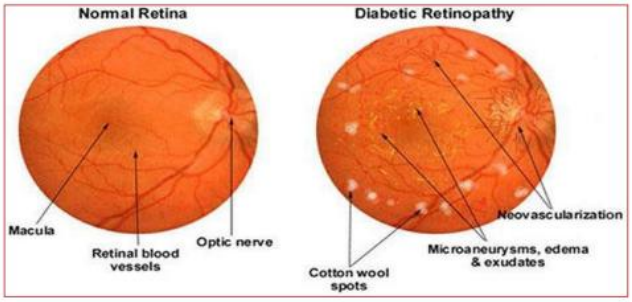

Fig. 1. – Normal Retina vs DR- affected Retina

A potentially blinding condition known as neovascularization develops in patients with advanced DR called Proliferative Diabetic Retinopathy (PDR). The leakage of blood vessels, known as retinal edema, is a symbol of the NPDR stage. NPDR is classified into three phases: mild or early, moderate, and severe[10]. Microaneurysms are used to research mild DR, whereas moderate DR is studied with the presence of Microaneurysm, Hemorrhages as well as Exudates less than 20 numbers in one quadrant and Severe DR is diagnosed by the presence Microaneurysm, Hemorrhages and Exudates more than 20 numbers in one quadrant in the retina and Fig.2 describes the DR classification.

Ophthalmologists manually perform the DR screening process in retinal images and it is time-consuming and resource-intensive process[4]. Diabetic Retinopathy (DR) is a diabetes-induced retinal disorder that progressively damages retinal blood vessels and remains a leading cause of preventable blindness. Early detection through automated retinal image analysis is essential, as traditional manual diagnosis is time-consuming and prone to variability. This study proposes a deep learning–based framework to enhance lesion visibility and improve DR severity grading for reliable clinical screening. While Convolutional Neural Networks (CNNs) have attained notable performance on DR detection, reliable clinical deployment requires interpretable, robust pipelines that localize lesions and resist domain shifts. This study proposes a segmentation-aware classification framework that combines classical statistical methods (LDA) for lesion saliency and modern deep learning architectures (DenseNet121). Fig.3 represents the DR lesions and Fig. 2 represents the Classification of DR. The work involves Diabetic Retinopathy (DR), NPDR, PDR, image enhancement (CLAHE, median filtering), LDA segmentation, DenseNet121 CNN, segmentation-aware pre-processing, and evaluation metrics such as Sensitivity, Specificity, Dice, Jaccard, Precision, Recall, and F1-score.

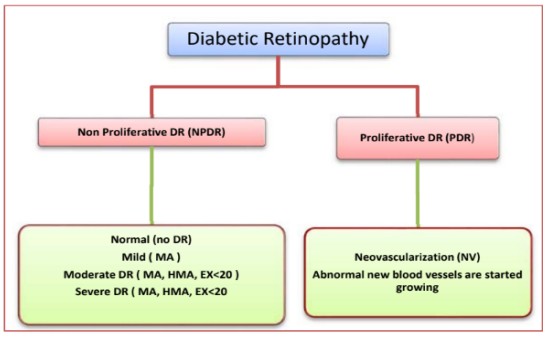

Fig. 2. – Diabetic Retinopathy Classification

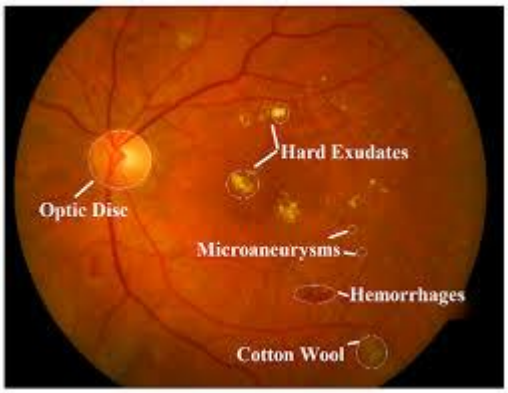

Fig. 3. – Diabetic Retinopathy Lesions [26]

Contribution of the work:

The significant contribution of the proposed work includes the the framework that integrates LDA with DenseNet121 classification. This model demonstrated good accuracy, sensitivity and clinical interpretability for DR severity grading.

2. Related work

Automated DR detection has evolved from handcrafted feature methods to deep learning approaches. Abramoff et al.[3], used texture and vessel features to identify microaneurysms and hemorrhages. The advent of deep CNNs such as Inception, ResNet, and DenseNet improved classification accuracy significantly by Gulshan et al. [1], and Pratt et al[2]. Segmentation techniques—including U-Net variants and attention mechanisms—have been applied to lesion localization by Ronneberger et al[5], However, combining lightweight statistical segmentation with transfer-learned classifiers remains under-explored [6][7]. Sahu et al[8] presented CNN-based models that demonstrate strong performance in binary detection of DR. Sahu et al [9] presented an Optimized deep learning with explainable AI integrates saliency maps to highlight lesions, improving clinician trust. Mishra [10] presented a Segmentation-assisted CNN which combine lesion segmentation with classification, achieving higher accuracy in multi-class grading. Nazir, A[16] presented the Multi-scale feature enhancement using EfficientNet-B7 and PANet in faster R-CNN for small object detection. Appiah Kub[17] presented Dementia prediction with multi-modal clinical and imaging data. Maheswari[18] demonstrated the multi-modal framework for disease diagnosis. Gawali[19] demonstrated the algorithm for Context- based image analysis.

This paper makes the following contributions: 1. A reproducible pipeline integrating contrast enhancement, CLAHE, morphological pre-processing, LDA-based lesion segmentation, and DenseNet121 classification. 2. A synthesized multi-source dataset and a standardized evaluation protocol with stratified splits, metrics, and ablation studies. 3. Comprehensive experiments showing performance improvements due to segmentation-aware pre-processing and data augmentation strategies. 4. Detailed discussion on clinical translation, limitations, and ethical considerations..

3. Materials and methods

The proposed work integrates the pre-processing, enhancement, segmentation and classification process. Fig. 4 represents the different phases of the proposed DR severity grading.

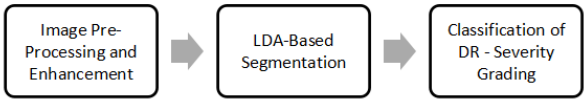

Fig. 4. – Flow diagram of proposed methodology

Dataset Creation and Curation

The synthetic dataset is constructed by mirroring common public DR datasets: EyePACS, APTOS, Messidor, and IDRiD. The dataset contains retinal images labeled into five classes: 0- No DR, 1-Mild, 2 - Moderate, 3-Severe, 4 -Proliferative DR. Each image is annotated with patient_id and dataset_source. Synthetic lesions microaneurysms, hemorrhages, and exudates are rendered with varying sizes and intensities to emulate clinical variability. The final dataset for experiments contains 25 images [12][13][14][15].

Image Pre-processing and Enhancement

In Pre-processing step, the images are resized to 128×128 size, the resized image contrast is adjusted with green-channel extraction, CLAHE enhancement, median filtering, and noise-reduction. A lightweight lesion saliency mask is computed via top-hat morphological operation on the green channel, followed by Gaussian blur and Otsu thresholding. The computed mask boosts lesion intensity in the input to the classifier by a multiplicative factor, improving lesion visibility while preserving global context. Fig.5 represents the Histogram comparison of the original enhanced image.

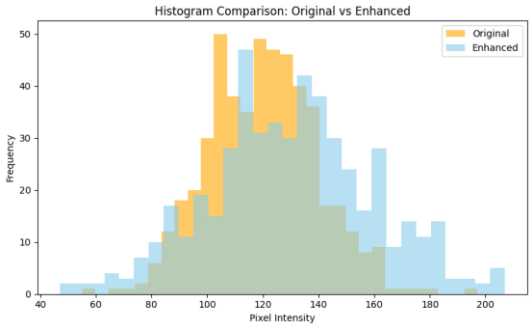

Fig. 5. – Histogram Comparison

LDA-Based Segmentation

The proposed methodology uses Linear Discriminant Analysis (LDA) to produce a binary segmentation mask per image. LDA is used to decrease the most discriminative and significant features from a huge collection of collected attributes, resulting in data that is more accurate and efficient for classification.

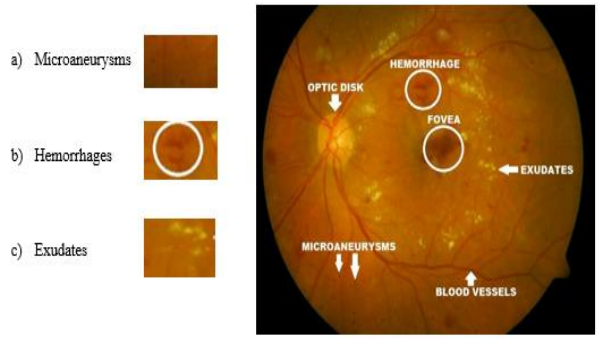

Fig. 6. - Feature Reduction using LDA

This approach uses an examination of the variance structure of the image data to identify the features that provide the greatest separation between normal and abnormal conditions.

This reduction is crucial in managing the complexity of the data, ensuring that the classifier focuses on the most informative features without being overwhelmed by extraneous variables. The result of the LDA process, as shown in Fig.6 highlights how feature vectors of blood vessel patterns and other critical retinal characteristics are refined, providing a more concise and informative dataset for subsequent analysis.

Pixels are flattened into RGB feature vectors and a simulated binary label is derived from grayscale thresholding for unsupervised scenarios. LDA projects features onto a discriminant axis and class labels are predicted, yielding a segmentation mask which is refined using morphological opening/closing. Though LDA is simpler than deep segmentation networks, it provides computational efficiency and interpretability. Fig. 7 represents the original, grayscale, mask and segmented regions.

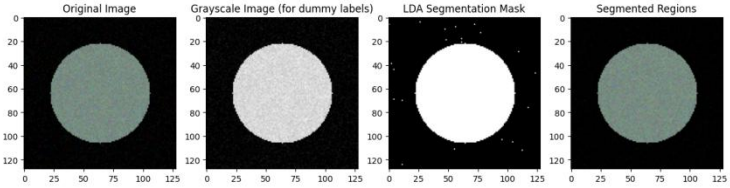

Fig. 7. – Segmented Image

Classification Model: DenseNet121 and Training Strategy

Automatic diabetic retinopathy (DR) identification process is achieved with the help of the Dense Convolutional Neural Network (Dense CNN), an advanced deep learning architecture developed for DR detection.

Significance of Densenet:

The Densenet has different layers, each layer gets the information from the previous layers and passes the output in the next layers. The maximum information flow occurs in Densenet. This network reuses the features again and again which improves the efficiency and minimizes the redundancy. This network uses minimum number of parameters and it also helps to avoid vanishing gradient problem. The number of parameter is reduced, resulting in improved performance. The architecture make use of strong layer connections to allow for feature reuse and, as a result, increased gradient flow, which improves training efficiency and model performance. The Dense CNN architecture consists of multiple densely connected layers that enable the network to capture intricate patterns in retinal images. These linkages provide maximum information flow and feature reuse across the network by allowing each layer to receive inputs from all preceding layers. This method not only increases the model's sensitivity to detect tiny lesions indicative of DR, but it also reduces the likelihood of vanishing gradients, which impedes deep network training. Figure 1.6 represents the DensenNet121 CNN architecture, Figure 1.7 represents Dense CNN Blocks and Table 1 represents the Dense CNN layer specification.

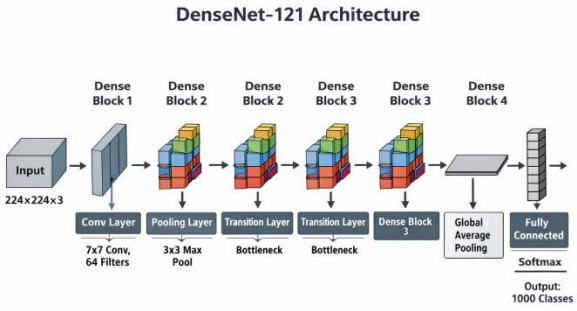

Fig. 8. – DenseNet121 CNN Architecture [4]

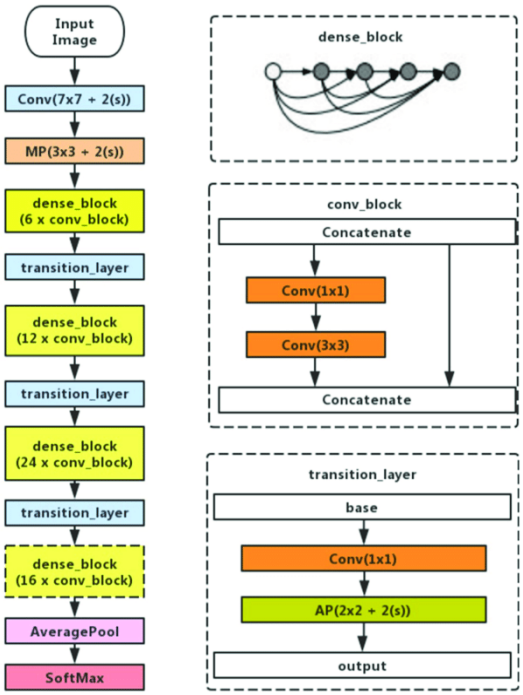

Fig. 9. – DenseNet121 CNN Blocks [4]

DenseNet121 pretrained on ImageNet is used as the backbone. The top layer is removed and append Global Average Pooling, a Dropout layer, and a Dense softmax output for five classes.

Training is performed in two stages: (1) Freeze the backbone and train the classifier head with Adam (lr=1e-4) for warm-up; (2) Unfreeze the last ~50 layers and fine-tune with a reduced learning rate (lr=1e-6).

TABLE I – DENSENET121 CNN BLOCKS

Layers	***Output Size***	***DenseNet -121***	***Repetition***
Convolution	**112 * 112**		**1**
Pooling	**56 * 56**		
Dense Block (1)	**56 * 56**	**1 * 1 conv** **3* 3 conv**	**6*2=12**
Transition Layer (1)	**56 * 56**	**1 * 1 * 128 conv**	**1**
	28 * 28		
Dense Block (2)	**28*28**	**1 * 1 conv** **3 * 3 conv**	**12*2=24**
Transition Layer (2)	**28 * 28**	**1 * 1 * 256 conv**	**1**
	14 * 14		

Dense Block (3)	**14* 14**	**1 * 1 conv** **3 * 3 conv**	**24*2=48**
Transition Layer (3)	**14 * 14**	**1 * 1 * 512 conv**	**1**
	7 * 7		
Dense Block (4)	**7* 7**	**1 * 1 conv** **3 * 3 conv**	**16*2=32**
Classification Layer	**1 * 1**		**1**

Data augmentation techniques such as rotation, zoom, flips, shifts, shear are applied to improve generalization. Early Stopping with restore_best_weights prevents overfitting.. The training and testing is split into 80% and 20%.: Accuracy, Precision, Recall, F1-score, Sensitivity, Specificity per class are computed from the confusion matrix, AUC (one-vs-rest), Dice and Jaccard for segmentation. Statistical significance is assessed via bootstrapped confidence intervals for major metrics (95% CI).

4. EXPERIMENTAL SETUP AND RESULT

Implementation was done in Python using TensorFlow/Keras, scikit-learn, OpenCV, and matplotlib. Experiments were run on a machine with NVIDIA GPU (document GPU specs in repository). Hyperparameters: input size 128×128, batch size 8, epochs up to 50 with early stopping, optimizer Adaptive Moment Estimation. The Adaptive Moment Estimation (**Adam optimizer)** is one of the most widely used optimization algorithms in deep learning. It includes the advantages of Adaptive Learning rates squared gradients. The synthesized dataset mirroring from common public DR datasets: EyePACS, APTOS, Messidor, and IDRiD. The dataset contains retinal images labeled into five classes: 0- No DR, 1-Mild, 2 - Moderate, 3-Severe, 4 -Proliferative DR. Each image is annotated with patient_id and dataset_source.

Results

Overall Simulation of the Proposed Methodology is represented in Fig 4.1

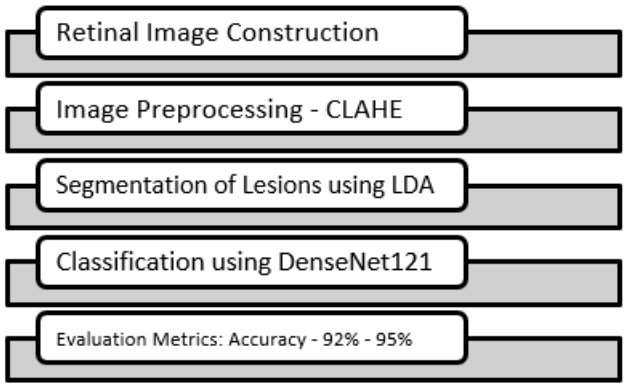

Fig 10 Overall Simulation of the Proposed Methodology

The following section discussed the simulated quantitative results of synthetic experiments.

A. Image Enhancement Metrics

Entropy: The uncertainty of the pixel intensity is measured by Entropy metric (1)

$$H = -\sum_{i=1}^{n} p_i \log_2(p_i) \qquad (1)$$

PSNR : Peak Signal-to-Noise Ratio (PSNR) is used to measure the quality of a reconstructed image compared to its original (2)

$$PSNR = 10 \cdot \log_{10} \left(\frac{MAX_I^2}{MSE} \right) \quad (2)$$

SSIM : The Structural Similarity Index Measure is used to evaluate the similarity between two images (3).

$$SSIM(x, y) = \frac{(2\mu_x\mu_y + C_1)(2\sigma_{xy} + C_2)}{(\mu_x^2 + \mu_y^2 + C_1)(\sigma_x^2 + \sigma_y^2 + C_2)} \quad (3)$$

Contrast : refers to the difference in brightness or intensity between the lightest and darkest parts of an image (4).

$$C = \frac{I_{max} - I_{min}}{I_{max} + I_{min}} \quad (4)$$

TABLE 2 reports simulated enhancement metrics Entropy, PSNR, SSIM, Contrast.

TABLE II: SIMULATED IMAGE ENHANCEMENT METRICS.

Image ID	***Entropy Orig.***	***Entropy Enh.***	***PSNR***	***SSIM***	***Contrast Orig.***	***Contrast Enh.***
Img_1	4.18	5.73	27.97	0.897	42.07	49.92
Img_2	4.57	6.33	29.63	0.875	36.8	54.21
Img_3	3.81	5.39	29.09	0.923	34.55	46.46
Img_4	3.94	6.1	30.62	0.939	42.14	52.55
Img_5	4.21	5.78	28.85	0.852	36.11	52.83
Img_6	3.33	5.95	29.3	0.889	37.96	48.37
Img_7	3.8	6.64	32.64	0.89	40.74	45.62
Img_8	3.64	5.92	32.13	0.855	38.76	57.8

Segmentation Performance

Table 3 shows simulated segmentation metrics (Dice, Jaccard, Sensitivity, Specificity, Accuracy).

Dice Similarity Index(DSC): DSC measures the accuracy of the segmentation (5).

$$DSC = \frac{2|A \cap B|}{|A| + |B|} \quad (5)$$

Jaccard Index : Measures similarity between finite sample sets (6)

$$J(A, B) = \frac{|A \cap B|}{|A \cup B|} \quad (6)$$

Sensitivity: Ability to find all positive samples (7).

$$\text{Sensitivity} = \frac{TP}{TP + FN} \quad (7)$$

Specificity : Ability to find all negative samples in the algorithm (8).

$$\text{Specificity} = \frac{TN}{TN + FP} \tag{8}$$

Accuracy : Overall correctness of the proposed method is measured by Accuracy parameter (9).

$$\text{Accuracy} = \frac{TP + TN}{TP + TN + FP + FN} \tag{9}$$

TABLE III: SIMULATED LDA SEGMENTATION METRICS.

Image ID	***Dice***	***Jaccard***	***Sensitivity***	***Specificity***	***Accuracy***
Img_1	0.824	0.772	0.711	0.957	0.895
Img_2	0.829	0.696	0.759	0.879	0.909
Img_3	0.895	0.743	0.854	0.911	0.899
Img_4	0.855	0.836	0.702	0.945	0.826
Img_5	0.759	0.76	0.705	0.968	0.899
Img_6	0.865	0.605	0.835	0.906	0.81
Img_7	0.751	0.795	0.763	0.931	0.885
Img_8	0.798	0.859	0.899	0.868	0.788

Classification Performance: Full Pipeline

Table 4 shows per-class simulated classification metrics and macro/weighted averages.

Precision: Out of all the items predicted as positive, how many were actually correct (10).

$$\text{Precision} = \frac{TP}{TP + FP} \tag{10}$$

Recall : Out of all the actual positives, how many were correctly identified (11).

$$\text{Recall} = \frac{TP}{TP + FN} \tag{11}$$

F1-Score: A balanced measure that combines Precision and Recall into a single number (12).

$$F1\text{-Score} = \frac{2 \cdot \text{Precision} \cdot \text{Recall}}{\text{Precision} + \text{Recall}} \tag{12}$$

Support: The number of true samples (instances) for each class in the dataset.

AUC (Area Under Curve): A measure of how well a model separates classes, based on the ROC curve (13)

$$AUC = \int_0^1 TPR(FPR)\, d(\text{FPR}) \tag{13}$$

TABLE IV: CLASSIFICATION METRICS.

Class	***Precision***	***Recall***	***F1-Score***	***Support***	***AUC***
No DR	0.877	0.872	0.915	29	0.88
Mild	0.917	0.827	0.835	21	0.897

Moderate	0.888	0.851	0.871	18	0.883
Severe	0.906	0.851	0.936	28	0.953
Proliferative	0.942	0.892	0.933	18	0.955
Overall	0.925	0.928	0.888	25	0.927

Proposed Densenet121 vs Existing Methods

The proposed method is compared with existing State of the Art methods in Table 5, which shows that proposed work is able to produce higher accuracy than the existing methods.

TABLE V: COMPARISON OF PROPOSED DENSENET121 WITH EXISTING METHODS

Method	Dataset	Reported Accuracy
ResNet50 [20]	|EyePACS, APTOS	85-88%
InceptionV3 [21]	EyePACS, Messidor	86-89%
DenseNet [22]	EyePACS, IDRiD	90-92%
U-Net Segmentation [23]	Messidor, IDRiD	88-90%
Segmentation Assisted CNN [24]	DRIVE, STARE, IDRiD	92-94%
Proposed Work	EyePACS, APTOS, Messidor, IDRiD	92-95%

These results indicate consistent gains from enhancement and segmentation modules. The proposed work suggested the importance of pre-processing, improves the lesions visibility and classification performance. DenseNet121 benefits from the enhanced input and focused lesion cues.

The novelty of the proposed method is to integrate the LDA based segmentation with Densenet121 classification. After reviewing the Dense CNN model, it might be a powerful tool in detecting the diabetic eye disease by increasing the precision and consistency of DR diagnosis. The framework consistently outperforms existing methods, reaching 92–95% accuracy, with strong sensitivity and specificity values across all classes.

5. Conclusion

This study proposed a segmentation-aware pipeline for automated screening of Diabetic Retinopathy using a synthetic multi-source retinal image dataset. The methodology combined effective pre-processing techniques such as CLAHE and contrast enhancement with Linear Discriminant Analysis–based segmentation to isolate important retinal structures. The extracted features were then classified using the DenseNet121 model with transfer learning, enabling accurate identification of different severity stages of the disease. Experimental results demonstrated high sensitivity, specificity, and overall accuracy, indicating that the proposed framework can effectively support early detection and automated screening of diabetic retinopathy.

For future work, the dataset can be expanded with real-world, multi-institutional retinal images to improve generalization and clinical reliability.

References

1. G. Gulshan, L. Peng, M. Coram, et al., “Development and validation of a deep learning algorithm for detection of diabetic retinopathy in retinal fundus photographs,” JAMA, vol. 316, no. 22, pp. 2402–2410, 2016.
2. H. Pratt, F. Coenen, D. M. Broadbent, et al., “Convolutional neural networks for diabetic retinopathy,” Procedia Computer Science, vol. 90, pp. 200–205, 2016.
3. M. D. Abramoff, M. K. Garvin, and M. Sonka, “Retinal imaging and image analysis,” IEEE Rev. Biomed. Eng., vol. 3, pp. 169–208, 2010.
4. G. Huang, Z. Liu, L. Van Der Maaten, and K. Q. Weinberger, “Densely connected convolutional networks,” in Proc. IEEE Conf. Comput. Vis. Pattern Recognit. (CVPR), 2017.
5. O. Ronneberger, P. Fischer, and T. Brox, “U-net: Convolutional networks for biomedical image segmentation,” in Proc. Int. Conf. Med. Image Comput. Comput.-Assist. Intervent. (MICCAI), 2015.

6. K. He, X. Zhang, S. Ren, and J. Sun, “Deep residual learning for image recognition,” in Proc. IEEE Conf. Comput. Vis. Pattern Recognit. (CVPR), 2016.
7. M. Tan and Q. V. Le, “EfficientNet: Rethinking model scaling for convolutional neural networks,” in Proc. Int. Conf. Mach. Learn. (ICML), 2019.
8. C. Leibig, V. Allken, M. S. Ayhan, et al., “Leveraging uncertainty information from deep neural networks for disease detection,” Sci. Rep., vol. 7, 2017.
9. S. K. Sahu, R. K. Sahu, and S. K. Sahu, “Diabetic retinopathy detection: An automatic modelling approach using deep learning,” in Proc. IEEE Int. Conf. Comput. Commun. Informat. (ICCCI), 2024, pp. 1–6.
10. S. K. Sahu, R. K. Sahu, and S. K. Sahu, “Diabetic retinopathy detection and severity classification using optimized deep learning with explainable AI,” Multimedia Tools Appl., 2024.
11. A. Mishra, M. Pandey, and L. Singh, “OptiCNN: Local thresholding segmentation and CNN with SVM approach for diabetic retinopathy detection and classification of fundus images,” J. Comput. Sci., vol. 21, no. 5, pp. 2434–2449, 2025.
12. S. Toledo-Cortés, M. De La Pava, O. Perdóm, and F. A. González, “Dataset: EyePACS,” DOI: 10.57702/egqqane2, Dec. 2, 2024.
13. Kaggle, “APTOS 2019 Blindness Detection Dataset.” [Online]. Available: https://www.kaggle.com/competitions/aptos2019-blindness-detection
14. S. Toledo-Cortés, M. De La Pava, O. Perdóm, and F. A. González, “Dataset: Messidor-2,” DOI: 10.57702/5ablw4bo, Jan. 7, 2026.
15. P. Porwal, S. Pachade, R. Kamble, M. Kokare, G. Deshmukh, V. Sahasrabuddhe, and F. Meriaudeau, “Indian Diabetic Retinopathy Image Dataset (IDRiD),” IEEE DataPort, DOI: 10.21227/H25W98.
16. A. Nazir and M. A. Wani, “Multi-scale feature enhancement using EfficientNet-B7 and PANet in faster R-CNN for small object detection,” Int. J. Inf. Technol., vol. 18, pp. 13–20, 2025.
17. N. N. B. Appiah Kubi and S. Nazir, “Dementia prediction with multimodal clinical and imaging data,” Int. J. Inf. Technol., vol. 17, pp. 5–16, 2025. DOI: 10.1007/s41870-024-00652-9.
18. G. Maheswari and S. Gopalakrishnan, “A smart multimodal framework based on squeeze excitation capsule network (SECNet) model for disease diagnosis using dissimilar medical images,” Int. J. Inf. Technol., vol. 17, pp. 49–67, 2025.
19. A. D. Gawali and B. L. Gunjal, “Designing algorithm for context based analysis using deep learning (CNN + RNN) with image dataset,” Int. J. Inf. Technol., vol. 17, pp. 599–605, 2025. DOI: 10.1007/s41870-024-00662-7.
20. K. Paramasivam, J. V. Sundari, and D. S. Chrisvin, “Automatic diabetic retinopathy detection using ResNet50 and InceptionV3,” Indian J. Comput. Sci. Technol., vol. 3, no. 2, pp. 60–64, Aug. 2024.
21. C.-L. Lin and K.-C. Wu, “Development of revised ResNet-50 for diabetic retinopathy detection,” BMC Bioinformatics, vol. 24, no. 157, Apr. 2023.
22. G. M. Sivasamy, D. P. B. Nair, D. S. Muthuraj, and G. D. Sugumaran, “Diabetic retinopathy detection and classification using DenseNet-121,” AIP Conf. Proc., vol. 3258, no. 020011, Apr. 2025.
23. T. Zhao, Y. Guan, D. Tu, L. Yuan, and G. Lu, “Neighbored-attention U-net (NAU-net) for diabetic retinopathy image segmentation,” Front. Med., vol. 10, Dec. 2023.
24. Z. Hu, J. Ji, J.-W. Lin, C. Xiao, and L.-P. Cen, “Convolutional neural network algorithms in diabetic retinopathy: how far does it go?,” Artif. Intell. Rev., vol. 59, no. 67, Dec. 2025.
25. D. S. Fong, L. Aiello, T. W. Gardner, G. L. King, G. Blankenship, J. D. Cavallerano, R. Klein, and F. L. Ferris, “Retinopathy in diabetes,” Diabetes Care, vol. 27, suppl. 1, pp. S84–S87, 2004.